# Imitation Refinement

**Junwen Bai**[1*], **Runzhe Yang**[1*], **Yexiang Xue**[1], **John Gregoire**[2], **Carla Gomes**[1]
[1] Cornell University
[2] California Institute of Technology
{jb2467,ry289,yx247}@cornell.edu, gregoire@caltech.edu, gomes@cs.cornell.edu,

## Abstract

Many real-world tasks involve identifying patterns from data satisfying background and prior knowledge, for which the ground truth is not available, but *ideal* data can be obtained, for example using theoretical simulations. We propose a novel approach, *imitation refinement*, which refines imperfect patterns by *imitating* ideal patterns. The imperfect patterns are obtained for example using an unsupervised learner. Imitation refinement *imitates* ideal data by incorporating prior knowledge captured by a classifier trained on the ideal data: an *imitation refiner* applies *small* modifications to imperfect patterns, so that the classifier can identify them. In a sense, imitation refinement fits the data to the classifier, which complements the classical supervised learning task. We show that our imitation refinement approach outperforms existing methods in identifying crystal patterns from X-ray diffraction data in materials discovery. We also show the generality of our approach by illustrating its applicability to a computer vision task.

## 1 Introduction

Many real-world tasks involve identifying meaningful patterns from data, satisfying background and prior knowledge [Chapelle *et al.*, 2009], for which not much labeled data are available. In such data-poor contexts, standard deep learning techniques are not effective, and therefore we need to rely on unsupervised learning. In many applications, *ideal data* can be obtained e.g., by synthesis and simulation [Rubin, 1993; Le Bras *et al.*, 2014]. In this paper, we explore how to use ideal data to incorporate background and prior knowledge into learning tasks.

As an example, consider the following application in materials science, where we would like to discover new materials, which are characterized by their X-ray diffraction (XRD) patterns, based on real experimental data. This identification problem is challenging because real XRD patterns often mix with others and are further corrupted with noise. Nevertheless, an *ideal* XRD pattern for a known material can be synthesized using theoretical simulations that incorporate prior knowledge about materials. Can we take advantage of synthesized *ideal* patterns to help discover unknown patterns corresponding to new materials from real experiments?

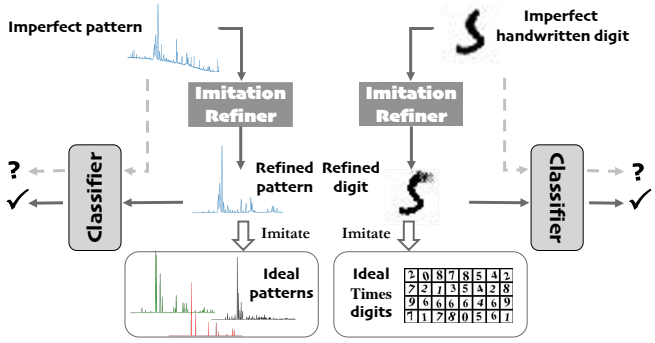


Figure 1: Imitation refinement improves the quality of imperfect patterns to *imitate* patterns in the ideal dataset. Left: Refinement of XRD crystal patterns. Right: Refinement of hand-written digits.

We give an affirmative answer in this paper. We propose a novel approach called *imitation refinement*, which improves the quality of imperfect patterns, obtained e.g., using an unsupervised learner from data, to *imitate* ideal, meaningful patterns, by incorporating prior knowledge captured by a classifier trained on the ideal dataset.

Imitation refinement applies *small* modifications to the imperfect patterns, so that a classifier, trained on the ideal dataset, identifies them. In a sense, imitation refinement fits the data to the classifier, which is inverse to supervised learning, where we fit a classifier to the data. In the materials discovery example, a classifier is trained using the synthesized ideal XRD dataset. Candidate patterns are obtained using an unsupervised learning method, from real experiments. Often, these patterns are imperfect. The imitation refiner applies small modifications to these patterns so that the classifier identifies them. As another example, we apply imitation refinement to hand-written digits, using ideal digits produced by different computer fonts. See Fig. 1.

Imitation refinement is related to data denoising [Xie *et al.*, 2012] and data restoration [Dong *et al.*, 2014], which improve noisy or corrupted data. One key difference is that imitation refinement does not require noisy data to be

[*] equal contribution

paired with its cleaned version while training. In fact, we directly train an imitation refiner on the imperfect dataset, for which we don't know the ground truth. Also, the ideal dataset does not provide ground truth counterparts for the imperfect data. Our work is also related to style transfer [Gatys *et al.*, 2015], which also requires paired images for the transformation. Besides, transfer learning [Pan and Yang, 2010] and domain adaptation [Glorot *et al.*, 2011] modify models while the classifier here is fixed. Additionally, imitation refinement has notable differences with conventional inverse classification [Mannino and Koushik, 2000; Aggarwal *et al.*, 2010], which uses inverted statistics to complete partial data or solve an optimization problem for each test sample respectively. Imitation refinement differs from these methods since it incorporates the knowledge embedded in a pre-trained classifier into the refiner, which can generalize to the unseen imperfect data. Further, imitation refinement allows for high-level data modification, while inverse classification often only changes data attributes. Finally, imitation refinement is different from GAN [Goodfellow *et al.*, 2014] since its goal is not to refine imperfect data such that a discriminator cannot differentiate them from ideal data. Instead, imitation refinement only applies small modifications to the imperfect data to reflect the fundamental characteristics of the ideal data, captured by the classifier trained on them.

Our contributions can be summarized as follows: (i) we propose a novel framework of imitation refinement, which improves the quality of imperfect patterns, by mimicking the characteristics of ideal data. (ii) We show that imitation refinement can be trained with neural nets and in an end-to-end fashion. (iii) We demonstrate the effectiveness of imitation refinement on two real-world applications: in the first application, we show imitation refinement improves the quality of poorly written digits by imitating typesetting or well-written digits. In the second application, we show that imitation refinement improves the quality of identified crystal patterns from X-ray diffraction data in materials discovery.

## 2 Problem Formulation

In imitation refinement, we have an *imperfect dataset* $A$, whose members come from post-processing a physical experiment or a complete unsupervised learning approach. Members in the imperfect dataset are defective because they fail to satisfy feasible conditions. On the other hand, we have an *ideal dataset* $E$, whose members satisfy all physical constraints and prior knowledge. Our question is how to modify the members in the imperfect dataset $A$ so that they imitate the characteristics of the members in the ideal dataset $E$. For example, in our materials discovery application, the imperfect dataset $A$ comprises of candidate patterns that are supposed to correspond to pure crystal structures that are obtained from real XRD data, using unsupervised learning. Each candidate pattern contains information of interest, but often it is mixed with other patterns or corrupted with background noise. On the other hand, we can obtain ideal XRD patterns for known materials from a dataset obtained using simulation. Such patterns are synthesized assuming ideal conditions. Our question is how we can fix the imperfect crystal structure patterns

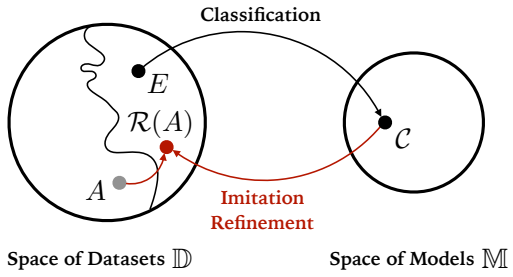


Figure 2: Imitation refinement is an inverse process of classification. In classification, we find an optimal classifier $\mathcal{C}$ on a fixed dataset $E$ (upper arc). In imitation refinement, we optimally refine the data to minimize the loss of a fixed classifier $\mathcal{C}$ (lower arc).

obtained by unsupervised learning to satisfy prior knowledge encapsulated in the ideal dataset.

Notice that we cannot complete this task by learning an one-to-one mapping between the imperfect dataset and the ideal dataset since the members of the imperfect dataset $A$ and ideal dataset $E$ refer to different entities. In our materials discovery application, members of the imperfect dataset $A$ correspond to potentially unknown materials from real experiments, while members of $E$ correspond to a restrictive set of theoretically synthesized and known materials. We cannot map any member in $A$ directly to a member in $E$. Instead, we modify members of the imperfect dataset $A$ so they have similar characteristics to those in the ideal dataset $E$.

We train an *ideal classifier* $\mathcal{C}$ to classify entities in the ideal dataset $E$, which captures the prior knowledge from an idealized world. The imitation refinement problem is to modify examples from the imperfect dataset $A$ so the classifier $\mathcal{C}$ identifies them. Formally, we search for an optimal refiner $\mathcal{R}$ to refine samples $x$'s drawn from the imperfect dataset $A$, such that $\mathcal{C}$ has better performance on the refined dataset $\mathcal{R}(A) = \{\mathcal{R}(x)|x \in A\}$. The performance of a classifier $\mathcal{C}$ is measured as its *evaluation loss*:

$$\eta_{\mathcal{C}}(A) := \mathbb{E}_{x\sim A}[\mathcal{H}(\mathcal{C}(x))], \tag{1}$$

where $\mathcal{H}(\cdot)$ is a function giving a low score if the refined examples can be certainly classified in one category in the ideal world. For instance, $\mathcal{H}(\cdot)$ can be the cross-entropy when the target categories are given when training, or be the entropy of predictions for some categories, which represents the uncertainty of the ideal classifier $\mathcal{C}$ on the refined dataset $R(A)$, in the non-targeted case. We expect a low $\eta_{\mathcal{C}}(\mathcal{R}(A))$ after refinement. Imitation refinement can be interpreted as an inverse process of supervised learning, as shown in Figure 2. In imitation refinement, we modify imperfect data $A$ to fit the classifier $\mathcal{C}$, instead of fitting a classifier to a fixed dataset.

Also, $\mathcal{R}$ should modify the original data as little as possible to accomplish its goal. We thus introduce a *discrepancy distance*:

$$\delta_{\mathcal{C}}(A, \mathcal{R}(A)) := \mathbb{E}_{x\sim A}[\delta_{\mathcal{C}}(x, \mathcal{R}(x))] \tag{2}$$

In general, $\delta_{\mathcal{C}}$ is a differentiable user-defined metric which measures the degree to which $\mathcal{R}$ modifies $x$. One option is to use a metric on the input space such as $\ell_p$ norm. In some

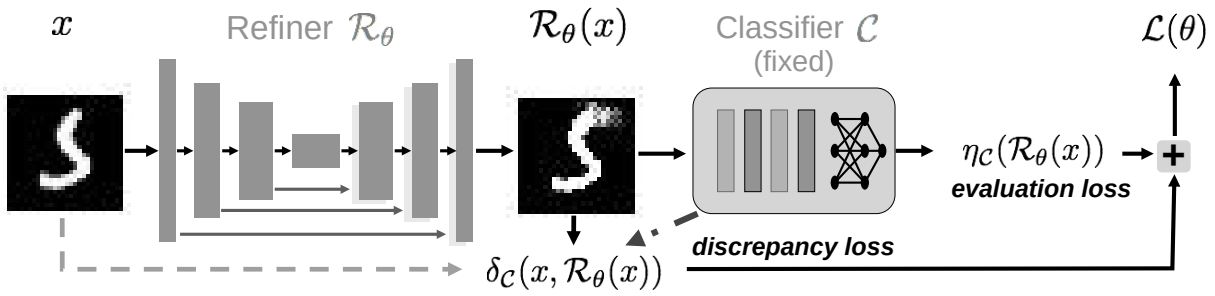


Figure 3: Network structure of neural imitation refinement.

cases, a distance metric based on higher level features can be more meaningful, such as features extracted from intermediate layers from a neural network.

Given the definition of evaluation loss and discrepancy distance, imitation refinement can be formulated as follows:

$$\min_{\mathcal{R}} \quad (1-\lambda)\delta_{\mathcal{C}}(A, \mathcal{R}(A)) + \lambda\eta_{\mathcal{C}}(\mathcal{R}(A)), \tag{3}$$

where $\lambda$ is a weight that trades off the refinement simplicity and evaluation loss.

## 3 Neural Imitation Refinement

We propose an end-to-end neural network based framework to solve the imitation refinement problem (3). Figure 3 illustrates the basic structure. The classifier $\mathcal{C}$ is pre-trained on the ideal dataset and is fixed during the training of refiner $\mathcal{R}$, parameterized by $\theta$. $x$ is the imperfect data drawn from $A$ to be refined. It first passes the refiner and becomes the refined data $\mathcal{R}_\theta(x)$. The evaluation loss $\eta_{\mathcal{C}}$ given by $\mathcal{C}$ is calculated on the input refined data $\mathcal{R}_\theta(x)$. The discrepancy distance $\delta_{\mathcal{C}}(x, \mathcal{R}_\theta(x))$ is calculated by comparing the refined $\mathcal{R}_\theta(x)$ with the original data $x$. In experiments, we first map both $x$ and $\mathcal{R}_\theta(x)$ to a high dimensional space denoted by a high-level layer of the classifier $\mathcal{C}$, and then use an $l_p$ norm in the high-level space to compute $\delta_{\mathcal{C}}$. The total loss to minimize is a trade-off between the evaluation loss and the discrepancy distance, $\mathcal{L}(\theta) = (1-\lambda)\cdot\delta_{\mathcal{C}} + \lambda\cdot\eta_{\mathcal{C}}$. Assuming that the given classifier is differentiable, a neural refiner $\mathcal{R}_\theta$ can be trained using stochastic gradient descent (see Algorithm 1).

**Classifiers** Our imitation refinement framework is highly flexible and can incorporate any classifiers that are differentiable. For the first handwritten digits application, we use a CNN-based model, LeNet [LeCun *et al.*, 1998], as the classifier. For the second materials discovery application, we use a RNN-based classifier, LSTM [Hochreiter and Schmidhuber, 1997], which achieves the best empirical result.

**Refiners** The refiner improves the given imperfect input and produces a refined input to be fed into the classifier. An end-to-end model is ideal for this purpose. Here we employ U-Net [Ronneberger *et al.*, 2015] to be our refiner (see Figure 3). The U-Net architecture is an encoder-decoder network which adds skip connections between encoder and decoder layers. The low-level and mid-level representations can be transferred to the decoders for up-sampling through these connections. We choose U-Net in our experiments because of good empirical performance. We expect other end-to-end models to work as well.

**Algorithm 1** Neural Imitation Refinement

Given the *ideal* classifier $\mathcal{C}$ and the imperfect dataset $A$.

**for** number of training iterations **do**

  Sample a minibatch $\{\boldsymbol{x}^{(1)}, \ldots, \boldsymbol{x}^{(m)}\}$ from $A$.

  Calculate $\delta_{\mathcal{C}}(\boldsymbol{x}^{(i)}, \mathcal{R}_\theta(\boldsymbol{x}^{(i)}))$ and $\eta_C(\mathcal{R}_\theta(\boldsymbol{x}^{(i)}))$ for $i \in [m]$ to estimate of loss functions (2) and (1).

  Update $\mathcal{R}_\theta$ by descending its stochastic gradient:

$$\nabla_\theta \frac{1}{m}\sum_{i=1}^{m}(1-\lambda)\delta_{\mathcal{C}}(\boldsymbol{x}^{(i)}, \mathcal{R}_\theta(\boldsymbol{x}^{(i)})) + \lambda\eta_{\mathcal{C}}(\mathcal{R}_\theta(\boldsymbol{x}^{(i)})),$$

**return** the refiner $\mathcal{R}_\theta$

## 4 Experiments

### 4.1 Hand-Written Digits

In this experiment, we first investigate the following question: if we have the ideal digits typeset in different fonts, can the imitation refinement take advantage of these idealized digits to refine unseen handwritten digits?

**Idealized Digit Datasets** We generate ideal datasets which contain images of digits typeset in five different fonts respectively: `Bradly Hand`, `Brush Script`, `Hannotate`, `Times`, and `Typewriter`. We augment images in each dataset by vertically and horizontally shifting at most two pixels, and also rotating in $\beta \in [-20°, 20°]$. Each dataset contains 10250 images of digits. We further add $10\%$ non-digit (mixtures of digits, etc.) images into each dataset, to satisfy the closed-world assumption. We also merge these five datasets to make a dataset `MixAll` containing digits typeset in all these fonts.

**Handwritten Digit Datasets** The MNIST dataset [LeCun *et al.*, 1998] is used as our imperfect dataset, which contains 60,000 handwritten digits for the training and validation and another 10,000 handwritten digits for the test. Some examples of digits in the *ideal* dataset and imperfect dataset are shown in the figure 4. Our goal is to refine handwritten digits by mimicking the characteristics of computer fonts.

**Classifiers Trained on Ideal Datasets** We first train the ideal classifiers on the idealized digit datasets. The classifiers should be able to classify instance in the idealized dataset into digits 0-9 and a `non-digit` category. The ideal classifiers are convolutional neural networks having the similar architecture

| | Bradly Hand | Brush Script | Hannotate | Times | Typewriter | MixAll |
|---|---|---|---|---|---|---|
| original non-digit rate | **0.78%** | 5.50% | 3.33% | 7.87% | 5.73% | 1.05% |
| refined non-digit rate | 0.01% | 0.01% | 0.14% | 0.01% | 0.07% | 0.08% |
| original accuracy | 39.20% | 48.18% | 48.38% | 47.89% | 40.25% | **83.28%** |
| refined accuracy | 98.72% | 98.49% | 98.40% | 98.56% | 98.01% | 98.27% |
| accuracy improvement | **+59.25%** | +50.31% | +50.02% | +50.67% | +57.76% | +14.99% |

Table 1: The improvement of identifiability of hand-written digits after imitation refinement. The first and second rows show the rates of handwritten digits regarded as non-digits in the test set before and after refinement, respectively. The third and fourth rows show the test accuracies of ideal classifiers on the original and refined MNIST test dataset. The ideal classifier trained on the dataset `MixAll` achieves the best accuracy. The huge improvements of accuracies show the refined handwritten digits can be better identified by ideal classifiers.

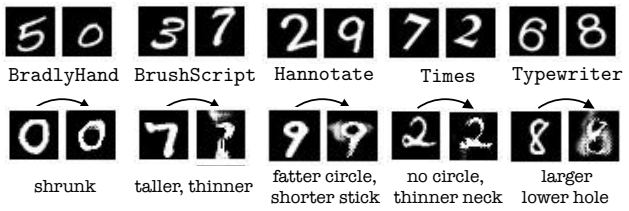


Figure 4: The first row displays example digits in the ideal dataset. The second row shows examples of imitatively refining MNIST handwritten digits to have the characteristics of different fonts.

with LeNet, which comprises two alternative convolutional layers and pooling layers for visual features extraction (32 and 64 filters of size $5 \times 5$ with padding stride 2 respectively, and max-pooling for each disjoint $2 \times 2$ area), and two fully connected layers with 1024 hidden units for output. These ideal classifiers achieve over $99.9\%$ test accuracy on their corresponding ideal datasets.

**Imitation Refiners** Then we train models similar to U-Net [Ronneberger *et al.*, 2015] as the refiners on the MNIST dataset with the help of prior knowledge captured by the ideal classifiers. When training, we consider two cases: a targeted case in which the labels of handwritten digits are given and a non-target case, otherwise. Notice that even in the target case, we don't know the ground truth of the handwritten digits while training, concerning the shape. In both cases the idealized counterparts of the digits are unknown. The evaluation loss $\eta_{\mathcal{C}}$ in the targeted case is the negative log-likelihood, and in the non-targeted case it is the entropy of digit predictions. The discrepancy distance $\delta_{\mathcal{C}}(x, \mathcal{R}(x))$ in this experiment is defined by the $\ell_1$-distance between the corresponding features maps extracted from the second convolutional layer of the classifiers. We set the $\lambda = 0.55$ in the objective function (3) to balance the refinement simplicity and effectiveness. An Adam optimizer with initial learning rate $10^{-4}$ is used to train the refiners with batch size 50 for total ten epochs.

## Experiment Results

**Improvement of accuracy** We show the improvement of identifiability of hand-written digits after imitation refinement in table 1. The 1st and 3rd rows present the rates of handwritten digits regarded as non-digits and test accuracies of ideal classifiers on the original MNIST test dataset before the refinement. The ideal classifier trained on the dataset `MixAll` achieves the best accuracy. Besides, the ideal classifier trained on the `Bradly Hand` dataset can better recognize the handwritten digits than other ideal classifiers since its original non-digit rate is low, but it poorly distinguishes 0-9 with $39.20\%$ accuracy. The 2nd and 4th rows show results after refinement. Refined handwritten digits can be better recognized by all these ideal classifiers, as the considerable improvement of accuracies indicates.

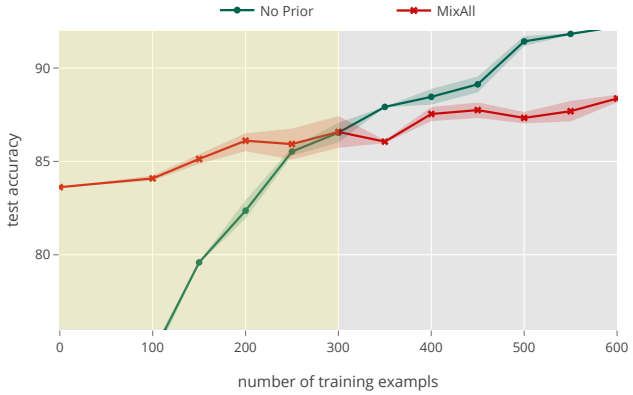


Figure 5: As the number of training examples from the MNIST dataset increases, the test accuracies of both ideal (`MixAll`) and real-world (`No Prior`) classifiers increase. However, when the number of the training examples is less than 300 (0.5% of MNIST), the captured prior knowledge can help the ideal classifier better recognize handwritten digits.

**The power of prior knowledge** We compare a *real world* classifier directly trained on the MNIST dataset with a ideal classifier trained on the idealized dataset `MixAll` in terms of test accuracy. The results are shown in figure 5. As the number of training examples from the MNIST dataset increases, the test accuracies of both ideal (`MixAll`) and real-world (`No Prior`) classifiers increase. In the long term, both of them will achieve over 98% test accuracies. However, when the number of the training examples is less than 300, the captured prior knowledge can help the refiner improve handwritten digits, so that the ideal classifier can better recognize them than the classifier without any prior knowledge.

**Visual effect of imitation refinement** To better illustrate the visual effect of imitation refinement, we also design a task to improve the poorly hand-written digits to mimic the well-written digits using imitation refinement. We use the same architectures for the classifier and refiner as in the previous setting. The ideal dataset contains the most representative well-written digits, which are manually selected from a sub-

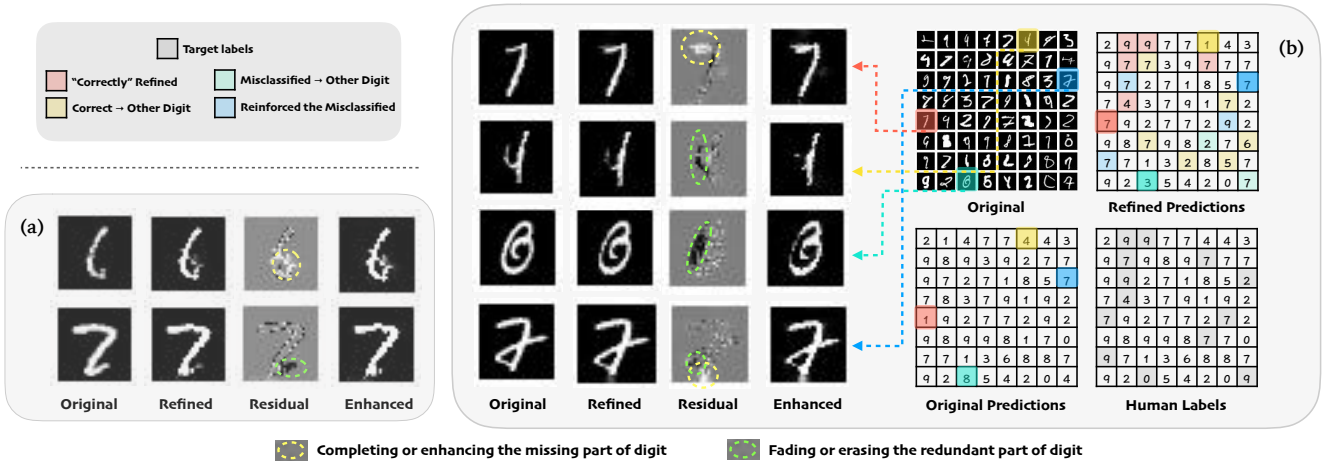


Figure 6: Visual results of imitation refinement: **(a)** Selected examples of test results of targeted refinement on the imperfect hand-written digits. We set $\lambda = 0.55$ in in the experiment to balance the discrepancy loss and the evaluation loss. In the first row, the target is "6" while the original imperfect digit is not complete. The refiner improves this digit by completing it. In the second row, the target is "7" while the original imperfect digit is like a "2". The refiner corrects this digit by erasing its redundant part. A more interesting example of a batch of test results of non-targeted imitation refinement on the poorly written digits is shown in **(b)**. The refiner modifies original ambiguous digits to the ones with higher classifier certainty. We set $\lambda = 0.15$ for this case. Since the process is non-targeted, it can creatively refine a digit to the less confusing one in the classifier's sense. Four interesting instances are displayed in the left figure: 1) The first row shows an imperfect digit originally classified as "1", being refined to a more idealized "7" by enhancing the horizontal line on the top, which corresponds with the human label. 2) The second row shows an imperfect digit correctly labeled originally as "4" but it may also be a "1" or "9", since its left part is blurred. By erasing its left part, it becomes a more certain "1". 3) An ambiguous digit which looks like "8", "3" and "0" is shown in the third row, whose human label is "0", while the classifier identifies it as "8". To increase the certainty, its left connected line is erased after refinement, and it is more like a digit "3". 4) In the last row, an imperfect digit "2" is so much like "7" that the classifier misclassified it. The refiner reinforces the classifier's opinion by extending the vertical line in the middle and fading the connecting line.

set of the MNIST dataset. We also manually select poor digits from another subset of the MNIST dataset, and the ground truths of these imperfect digits are unknown. When training, the discrepancy distance is the same as that in the previous setting. And the evaluation loss has two configurations: when the labels of digits are given when training the refiner (targeted case), it is the negative log-likelihood. Notice that it does not mean we know the ground truths of poor hand-written digits in terms of shape. The idealized well-written counterparts of the digits are still unknown. When the labels of the digits are not given (non-targeted case), it is the entropy of the prediction to be a digit, since we expect a poorly written digit to not be a `non-digit`, and increase the classifier's certainty after refinement. We show visual results in figure 6.

## 4.2 Materials Discovery

### Motivations and Modeling

In this second application, we further apply imitation refinement to a scientific task in *materials discovery*.

High throughput combinatorial materials discovery is a materials science task whose intent is to discover new materials using a variety of methods including X-ray diffraction pattern analysis [Green *et al.*, 2017] . Figure 7 shows a typical physically meaningful material system. In a ternary material composition space, different ratios of three metallic elements are mixed together to form different crystalline materials. At each elemental composition, also called sample, a different material is formed, which can be composed of a single crystalline compound, or a mixture of several compounds. The

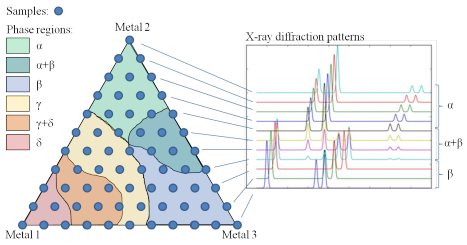


Figure 7: Materials discovery task: Each blue dot is a sample. $\alpha, \beta, \gamma$ represent different phases/compounds. The XRD pattern at each sample point is given, potentially a mixture of $\alpha, \beta, \gamma$. The goal is to obtain the unknown pure XRD patterns of $\alpha, \beta, \gamma$.

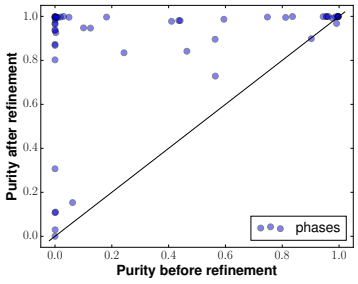


Figure 8: A blue dot at location $(x, y)$ denotes a phase whose purity is $x$ before refinement and $y$ after refinement.

X-ray diffraction (XRD) pattern at each sample is given. The goal is to unveil the XRD pattern of each single compound, which is also referred to as **"phase"**.

The above task can be modeled as a typical pattern decomposition problem under constraints, which was explored in recent work [Long *et al.*, 2009; Ermon *et al.*, 2015; Xue *et al.*, 2017; Suram *et al.*, 2016; Bai *et al.*, 2017]. Though these methods produce estimated patterns for each phase that are usually quite similar to the expected patterns of corresponding pure phases, they typically include a fraction of the patterns belonging to other phases, as well as background and experimental noise. This leads to errors in explaining the structure of the materials system, and the goal of this application is to refine each imperfect pattern to more correctly estimate that of the corresponding pure phase.

The *ideal* dataset $E$ in this application is composed of physically meaningful synthetic pure phases and mixtures from the Materials Project [Jain *et al.*, 2013]. The Materials Project provides crystal structure information and energy of formation using density functional theory for each phase. XRD patterns are calculated for each constituent using pymatgen [Ong *et al.*, 2013]. In this database, approximately 3000 synthetic material systems contain over 30,000 pure phases and 32,000 mixtures. 95% of the 3000 systems provide pure phases and mixtures used for creating the ideal dataset $E$ for training the classifier $\mathcal{C}$ to discriminate between pure phases and mixtures. Among these systems, 80% are picked randomly for training ($E_{train}$), while 10% are left for validation ($E_{valid}$) and another 10% for testing ($E_{test}$).

The imperfect dataset $A$ is derived from the remaining 135 systems. For each system, non-negative matrix factorization (NMF) [Lee and Seung, 2001] decomposed all the XRDs into phases that are supposed to be pure. Note however that typically they differ from the expected pure phases, as described above. These imperfect phases form the imperfect dataset $A$, which should be refined to be more pure. We randomly split $A$ into training set $A_{train}$ (80%), validation set $A_{valid}$ (10%) and test set $A_{test}$ (10%). We assume that the imperfect patterns $x$ in $A$ are pure phases, since they are the factors produced by NMF. Nevertheless, the ground-truth mapping $G(x)$, which matches each imperfect phase to the corresponding ground-truth pure phase, is not known during the training of the refiner. To simulate the real materials discovery where we explore new systems without ground truths based on known systems, $E$ contains all the known systems while $A$ comprises of unknown systems, which means $G(A_{train})$ is unused in training and $G(A_{test})$ is used only for evaluation.

$\delta_{\mathcal{C}}(x, \mathcal{R}(x))$ is the KL divergence, $D_{KL}(\mathcal{R}(x)||x)$, and $\eta_{\mathcal{C}}(\mathcal{R}(A))$ is the negative log-likelihood given by $\mathcal{C}$. A network similar to the previous application is used here except that $\mathcal{C}$ is an LSTM and $\mathcal{R}$ is adapted to process 1-d input.

### Training and Results

Each XRD pattern is of length 2000 and is further dissected into 50 segments, each of length 40. A simple one-layer LSTM with dropout 0.5 and hidden size 64 is used here for classification. The final output feature of cell state is fed into a softmax layer for classification. The batch size for training is 64. The LSTM gives 94.93% prediction accuracy on $E_{test}$.

| Methods | AgileFD | IAFD | NMF | IR |
|---|---|---|---|---|
| $\ell_1$ | 44.4230 | 45.7362 | 45.4367 | **43.9345** |
| $\ell_2$ | 0.1430 | 0.1373 | 0.1393 | **0.1197** |
| *KL div* | 76.8572 | 74.7262 | 78.1946 | **74.5778** |

Table 2: Comparisons with the ground-truth phases. For $\ell_1$ loss, $\ell_2$ loss and *KL divergence*, the smaller, the better. The best result for each measure is in **bold**. Imitation refinement (IR) uses NMF for generating imperfect dataset $A$.

The confidence of being recognized as pure phase by the classifier $\mathcal{C}$ is its *purity*. Figure 8 shows the purity before and after refinement: all the phases from $A_{test}$ get improved dramatically, except one in the upper-right corner. Even in the case where the initial purity is small indicating that the raw phase is not pure, many phases are still improved significantly (see the left upper corner in the figure).

We also evaluate the performance of the refiner $\mathcal{R}$ directly by the classification output of $\mathcal{C}$. Initially, $\mathcal{C}$ classified only 36.54% of the examples in $A_{test}$ as pure phases, but after refinement, this percentage goes to 88.46%.

We also evaluate the refined phases $R(A_{test})$ by comparing with the ground-truth $G(A_{test})$, using the $l_1$ loss, $l_2$ loss, KL divergence. Recall that neither $\mathcal{C}$ nor $\mathcal{R}$ were trained with paired imperfect and ground truth data, and $\mathcal{R}$ was trained only to increase purity as represented by $\mathcal{C}$. This evaluation is therefore much more challenging in that the refiner is not directly trained to minimize the difference, but the evaluation is also more relevant to the scientific discovery goals.

Imitation refinement is compared with NMF and another two state-of-art methods, AgileFD [Suram *et al.*, 2016] and IAFD [Bai *et al.*, 2017] on the quality of phases. The phases produced by these methods are compared with the corresponding ground truth. Different measurements are taken to evaluate them. For each type of measurement, the sum over the distances for all the testing phases are shown in the Table 2. Imitation refinement (IR) outperforms other methods or is at least as competitive as the others.

## 5 Discussion and Future Work

*Imitation refinement* improves the quality of imperfect data by imitating *ideal data*. Using the prior knowledge captured by an *ideal classifier* trained on an ideal dataset, a refiner learns to apply modifications to imperfect data, such that the ideal classifier can better recognize them. A general end-to-end neural framework is proposed to address the underlying optimization problem and it is further exemplified by two applications: handwritten digits and XRD patterns in materials discovery. Imitation refinement improves readability and accuracy of identifying hand-written digits when complementing a small training dataset (0.3% of MNIST) with computer generated data. It also improves the quality of crystal phases produced by an unsupervised learner (NMF), a promising result in scientific discovery. Imitation refinement is easily extensible with different ways of producing and refining the imperfect data. For example, imperfect data may result from crowdsourcing tasks to non-experts and other supervised models can be used. Imitation refinement is a promising approach for incorporating prior and background knowledge

into learning tasks. We hope that this work will stimulate additional imitation refinement efforts.

## References


[Aggarwal *et al.*, 2010] Charu C Aggarwal, Chen Chen, and Jiawei Han. The inverse classification problem. *Journal of Computer Science and Technology*, 25(3):458–468, 2010.

[Bai *et al.*, 2017] Junwen Bai, Johan Bjorck, Yexiang Xue, Santosh K Suram, John Gregoire, and Carla Gomes. Relaxation methods for constrained matrix factorization problems: Solving the phase mapping problem in materials discovery. In *International Conference on AI and OR Techniques in Constraint Programming for Combinatorial Optimization Problems*, pages 104–112. Springer, 2017.

[Chapelle *et al.*, 2009] Olivier Chapelle, Bernhard Scholkopf, and Alexander Zien. Semi-supervised learning (chapelle, o. et al., eds.; 2006)[book reviews]. *IEEE Transactions on Neural Networks*, 20(3):542–542, 2009.

[Dong *et al.*, 2014] Chao Dong, Chen Change Loy, Kaiming He, and Xiaoou Tang. Learning a deep convolutional network for image super-resolution. In *European Conference on Computer Vision*, pages 184–199. Springer, 2014.

[Ermon *et al.*, 2015] Stefano Ermon, Ronan Le Bras, Santosh K Suram, John M Gregoire, Carla P Gomes, Bart Selman, and Robert Bruce van Dover. Pattern decomposition with complex combinatorial constraints: Application to materials discovery. 2015.

[Gatys *et al.*, 2015] Leon A Gatys, Alexander S Ecker, and Matthias Bethge. A neural algorithm of artistic style. *arXiv preprint arXiv:1508.06576*, 2015.

[Glorot *et al.*, 2011] Xavier Glorot, Antoine Bordes, and Yoshua Bengio. Domain adaptation for large-scale sentiment classification: A deep learning approach. In *Proceedings of the 28th international conference on machine learning (ICML-11)*, pages 513–520, 2011.

[Goodfellow *et al.*, 2014] Ian Goodfellow, Jean Pouget-Abadie, Mehdi Mirza, Bing Xu, David Warde-Farley, Sherjil Ozair, Aaron Courville, and Yoshua Bengio. Generative adversarial nets. In *Advances in neural information processing systems*, pages 2672–2680, 2014.

[Green *et al.*, 2017] M. L. Green, C. L. Choi, J. R. Hattrick-Simpers, A. M. Joshi, I. Takeuchi, S. C. Barron, E. Campo, T. Chiang, S. Empedocles, J. M. Gregoire, et al. Fulfilling the promise of the materials genome initiative with high-throughput experimental methodologies. *Applied Physics Reviews*, 4(1):011105, 2017.

[Hochreiter and Schmidhuber, 1997] Sepp Hochreiter and Jürgen Schmidhuber. Long short-term memory. *Neural computation*, 9(8):1735–1780, 1997.

[Jain *et al.*, 2013] Anubhav Jain, Shyue Ping Ong, Geoffroy Hautier, Wei Chen, William Davidson Richards, Stephen Dacek, Shreyas Cholia, Dan Gunter, David Skinner, Gerbrand Ceder, et al. Commentary: The materials project: A materials genome approach to accelerating materials innovation. *Apl Materials*, 1(1):011002, 2013.

[Le Bras *et al.*, 2014] Ronan Le Bras, Richard Bernstein, John M Suram, Santosh K Gregoire, Carla P Gomes, Bart Selman, and R Bruce van Dover. A computational challenge problem in materials discovery: Synthetic problem generator and real-world datasets. 2014.

[LeCun *et al.*, 1998] Yann LeCun, Léon Bottou, Yoshua Bengio, and Patrick Haffner. Gradient-based learning applied to document recognition. *Proceedings of the IEEE*, 86(11):2278–2324, 1998.

[Lee and Seung, 2001] Daniel D Lee and H Sebastian Seung. Algorithms for non-negative matrix factorization. In *Advances in neural information processing systems*, pages 556–562, 2001.

[Long *et al.*, 2009] CJ Long, D Bunker, X Li, VL Karen, and I Takeuchi. Rapid identification of structural phases in combinatorial thin-film libraries using x-ray diffraction and non-negative matrix factorization. *Review of Scientific Instruments*, 80(10):103902, 2009.

[Mannino and Koushik, 2000] Michael V Mannino and Murlidhar V Koushik. The cost-minimizing inverse classification problem: a genetic algorithm approach. *Decision Support Systems*, 29(3):283–300, 2000.

[Ong *et al.*, 2013] Shyue Ping Ong, William Davidson Richards, Anubhav Jain, Geoffroy Hautier, Michael Kocher, Shreyas Cholia, Dan Gunter, Vincent L Chevrier, Kristin A Persson, and Gerbrand Ceder. Python materials genomics (pymatgen): A robust, open-source python library for materials analysis. *Computational Materials Science*, 68:314–319, 2013.

[Pan and Yang, 2010] Sinno Jialin Pan and Qiang Yang. A survey on transfer learning. *IEEE Transactions on knowledge and data engineering*, 22(10):1345–1359, 2010.

[Ronneberger *et al.*, 2015] Olaf Ronneberger, Philipp Fischer, and Thomas Brox. U-net: Convolutional networks for biomedical image segmentation. In *International Conference on Medical Image Computing and Computer-Assisted Intervention*, pages 234–241. Springer, 2015.

[Rubin, 1993] Donald B Rubin. Discussion statistical disclosure limitation. *Journal of official Statistics*, 9(2):461, 1993.

[Suram *et al.*, 2016] Santosh K Suram, Yexiang Xue, Junwen Bai, Ronan Le Bras, Brendan Rappazzo, Richard Bernstein, Johan Bjorck, Lan Zhou, R Bruce van Dover, Carla P Gomes, et al. Automated phase mapping with agilefd and its application to light absorber discovery in the v–mn–nb oxide system. *ACS combinatorial science*, 19(1):37–46, 2016.

[Xie *et al.*, 2012] Junyuan Xie, Linli Xu, and Enhong Chen. Image denoising and inpainting with deep neural networks. In *Advances in neural information processing systems*, pages 341–349, 2012.

[Xue *et al.*, 2017] Yexiang Xue, Junwen Bai, Ronan Le Bras, Brendan Rappazzo, Richard Bernstein, Johan Bjorck, Liane Longpre, Santosh K Suram, Robert Bruce van Dover, John M Gregoire, et al. Phase-mapper: An ai

platform to accelerate high throughput materials discovery. 2017.